

Geometrical branching model: A Monte Carlo simulation of multiparticle production

Rudolph C. Hwa and Ji-Cai Pan

Institute of Theoretical Science and Department of Physics, University of Oregon, Eugene, Oregon 97403-5203

(Received 20 May 1991)

The geometrical branching model for soft production in hadronic collisions is developed into a Monte Carlo code, called ECCO, in which the eikonal formalism is combined with cluster cascades. The model not only can account for the global features of multiparticle production, but is also designed to describe the properties of rapidity fluctuations in small rapidity bins. With the use of five parameters ECCO can simultaneously simulate all the data on $\langle n \rangle$, P_n , C_q , dn/dy , $C(y_1, y_2)$, dN/dp_T^2 , and F_q , for \sqrt{s} ranging from 10 to 65 GeV, nearly all within error bars.

PACS number(s): 13.85.Hd, 12.40.Pp

I. INTRODUCTION

The geometrical branching model (GBM) [1–3] is one among several models which include notably the dual parton model (DPM) [4,5] and the FRITIOF model [6], that are successful in describing the global features of multiparticle production in soft hadronic collisions [7]. However, until now the GBM has lacked a Monte Carlo (MC) code that can simulate the event structure of soft production. The aim of this paper is to amend that defect.

Another more important development of the GBM to be reported here is the sharpening of our ideas about the branching process. This is possible because experimental data on local properties that have become available only recently place severe demands on dynamical models. Here we refer to the phenomenology of intermittency in multiplicity fluctuations [8], first suggested by Bialas and Peschanski [9]. It quantifies the fluctuation of rapidity distribution in small rapidity intervals. Intermittent behaviors have been found in all hard and soft processes in nearly all collisions involving leptons, hadrons, and nuclei [10]. Whereas the Lund parton-shower model [11] has been able to account for the behavior in the hard processes of e^+e^- annihilation, no model with a MC code for soft production can generate the intermittency observed in hadronic collisions [8]. The code that we develop here for the GBM is tuned to fit the intermittency data, and therefore has the virtue of being able to account for all aspects of the hadronic data that we have brought to bear on the code. We have found that the intermittency data impose severe constraints on the branching process, thereby demonstrating the importance of studying intermittency.

II. A BRIEF REVIEW OF THE GBM

For $\sqrt{s} < 100$ GeV the GBM has been shown [1] to possess the observed properties of geometrical scaling, Koba-Nielsen-Olesen (KNO) scaling, and forward-backward multiplicity correlation. The inclusive distribution in rapidity has not been calculated because the model was not sufficiently well developed in the details of

the branching process [3]. At higher energies it is known that minijet production breaks the various scaling behaviors, and the GBM augmented by QCD hard subprocesses has successfully accounted for the changes in the above global properties [12]. Since we aim to concentrate in this paper only on the improvement of the soft production part of the model, deferring the hard processes to a future investigation, we shall limit the energy range of our consideration here to $10 < \sqrt{s} < 100$ GeV, which covers the CERN ISR range.

Let us first summarize the foundation of the GBM [1–3,12,13]. The geometrical part of the model refers to the eikonal formalism of hadronic collision at high energy. In terms of the eikonal function $\Omega(b)$ the elastic, inelastic, and total cross sections are

$$\sigma_{el} = \int d^2b (1 - e^{-\Omega(b)})^2, \quad (2.1)$$

$$\sigma_{inel} = \int d^2b (1 - e^{-2\Omega(b)}), \quad (2.2)$$

$$\sigma_{tot} = \int d^2b 2(1 - e^{-\Omega(b)}). \quad (2.3)$$

In the energy range of interest stated above there is geometrical scaling; i.e., σ_{el}/σ_{tot} is roughly constant [14]. That property can be guaranteed if Ω depends only on the scaled impact parameter R , where

$$R = b/b_0(s) \quad (2.4)$$

so that (2.1)–(2.3) may be written as

$$\sigma_{el} = \pi b_0^2(s) \int_0^\infty dR^2 (1 - e^{-\Omega(R)})^2, \quad (2.5)$$

$$\sigma_{inel} = \pi b_0^2(s) \int_0^\infty dR^2 (1 - e^{-2\Omega(R)}), \quad (2.6)$$

$$\sigma_{tot} = \pi b_0^2(s) \int_0^\infty dR^2 2(1 - e^{-\Omega(R)}). \quad (2.7)$$

The scale $b_0(s)$ is defined by requiring that $\sigma_{inel} = \pi b_0^2(s)$, so that the inelasticity function

$$g(R) = 1 - e^{-2\Omega(R)} \quad (2.8)$$

satisfies the normalization condition

$$\int_0^\infty dR^2 g(R) = 1. \quad (2.9)$$

$g(R)$ describes the probability of having an inelastic collision at R . Expanding it in a power series, we can write

$$g(R) = \sum_{\mu=1}^{\infty} \pi_{\mu}(R) \quad (2.10)$$

where

$$\pi_{\mu}(R) = \frac{[2\Omega(R)]^{\mu}}{\mu!} e^{-2\Omega(R)}. \quad (2.11)$$

The μ th-order term may be regarded as the μ th-order rescattering contribution, and for $\mu \geq 2$ it is important only when R is small; the exponential factor is the absorptive correction.

The eikonal formalism, of course, is quite general [15]. It satisfies unitarity, which relates elastic and inelastic scattering amplitudes. It emphasizes the spatial properties of an extended hadron, and in that respect differs from most other models on hadronic collisions, which are formulated in the momentum space. It is also consistent with Regge theory [16], in the framework of which π_1 corresponds to one cut Pomeron, π_2 two cut Pomerons, etc. However, the eikonal-Regge theory does not go beyond generalities to specify the detail characteristics of multiparticle production. Only models that are not based on first principles but are phenomenologically motivated can carry us further to a description of the properties of soft interaction. The GBM chooses to regard the soft production as a branching process, similar but not identical to the hard production process [17].

If at R the probability of producing n particles is $B_n(R)$, then the multiplicity distribution after impact-parameter smearing is

$$P_n = \int_0^{\infty} dR^2 g(R) B_n(R). \quad (2.12)$$

In a first attempt to model $B_n(R)$ in the framework of stochastic processes, $B_n(R)$ was expressed in terms of the Furry distribution F_n^k , which is the solution of the stochastic evolution equation for Furry branching with k sources [17,18]. It was shown then that with an appropriate R dependence of $k(R)$ the resultant P_n agrees well with the ISR data; it therefore possesses the KNO scaling property [1,19]. However, since F_n^k does not specify where the particles are produced in rapidity space, the branching process was underspecified. Nevertheless, the model so described was sufficient to be used as a basis for going on to higher energies to include minijet production [12] and to large systems involved in nuclear collisions [13].

When the GBM was first proposed, the aim was only to achieve both geometrical scaling and KNO scaling [1]. Soon after that the phenomenology of intermittency received intense attention, and it appeared clear that most existing dynamical models were unable to produce self-similarity in the rapidity fluctuations [8]. The α model of random cascading [9] suggests that a dynamical model based on branching is more likely to succeed. This idea has been put to test in specific model calculations, which indeed yield intermittency [20,21]. Thus the GBM has acquired a new mission, since its branching part is well poised to incorporate the appropriate mechanism for in-

termittency and forge a realistic dynamical model for soft production that exhibit both the global and local features of the experimental data.

In order to implement the branching process with actual steps of branching, a simple Monte Carlo simulation was attempted with the aim of reproducing the global features such as P_n in the full rapidity space [3]. Cluster cascading was considered in a scheme in which a specific mass spectrum was used. However, that mass spectrum has an exponential cutoff characterized by a ‘‘temperature,’’ which introduces a scale in the problem. It is therefore reasonable to suspect that such a branching scheme is not likely to lead to self-similarity in rapidity fluctuation.

In the next section we describe a MC code which yields results that agree not only with the global properties of the data, but also with intermittency at all scales of rapidity intervals. Being a first attempt in developing a MC code for GBM, we are still limited in our objectives. We shall work essentially in a one-dimensional phase space in our branching process, even though the p_T distribution will be considered. We shall not consider resonance production explicitly, nor keep track of the charges of the particles produced. By keeping the procedure simple, we hope to make clear the basic mechanism of particle production in our model.

III. MONTE CARLO SIMULATION BY ECCO

We now describe our MC code, called ECCO, which stands for eikonal cascade code.

For definiteness we consider pp collisions for which the eikonal function $\Omega(R)$ has been well determined from elastic scattering and has the indirect parametrization [22]

$$1 - e^{-\Omega(R)} = 0.71e^{-1.17R^2}. \quad (3.1)$$

Using this in supplement to (2.11) and (2.12) forms the eikonal basis of our approach. There are various issues that we must deal with in specifying the branching process. We now describe them separately.

A. Energy for particle production

Even at a fixed R the energy W involved in the production of particles fluctuates from event to event around an average that depends on R and \sqrt{s} . Since the proton-inclusive cross section ($p + p \rightarrow p + X$) as a function of the proton momentum fraction x is known to be rather flat [23], i.e., $d\sigma/dx$ is roughly constant, we know that the leading particles take away a large portion of \sqrt{s} . Indeed, the constancy of $d\sigma/dx$ implies that the mean momentum fraction of the proton, $\langle x \rangle_p$, is roughly $\frac{1}{2}$. That is after averaging over impact parameter. Hence, we expect $\langle W \rangle$ to be roughly $\sqrt{s}/2$, and the fluctuation of W from $\langle W \rangle$ is very large. W/\sqrt{s} should be large at small R , but small at large R .

The dependence of W on R should be through the eikonal function $\Omega(R)$. Since $\Omega(R)$ is the overlap function that describes the opacity of the colliding hadrons, more particles are likely to be produced at large $\Omega(R)$, so

more energy would be spent in producing those particles. Our model at this point does not specify the determination of the momenta of the leading particles, so we can only take \bar{W} for the production of mesons to dependent on $\Omega(R)$ in some simple manner. Since $\Omega(R)$ is an average quantity, it is actually the event-averaged \bar{W} , averaged over all collisions at R , that is to be related to $\Omega(R)$. We parametrize that relationship by the formula

$$\frac{\bar{W}}{\sqrt{s}} = \left(\frac{\Omega}{\Omega_0} \right)^\lambda \quad (3.2)$$

where $\Omega_0 = \Omega(R=0)$, and λ is a free parameter to be determined phenomenologically. The fluctuation of W from \bar{W} for any given event cannot be determined *a priori*; thus, it raises a question on the meaningfulness of conservation of energy in the branching process, when the initial energy of hadron production for each event is unknown. We shall return to this point later. We remark here that this is another aspect of the hadronic collision that is very different from e^+e^- annihilation, for which the initial energy is exactly the total energy for particle production in every event.

B. Cut Pomerons

In combining (2.10) and (2.11) with (2.12) in order to calculate the multiplicity distribution P_n , we improve the model by writing

$$P_n = \int_0^\infty dR^2 \sum_{\mu=1}^{\infty} \pi_\mu(R) B_n^\mu \quad (3.3)$$

where B_n^μ is introduced in recognition of the interpretation for each term in the series as an independent contribution from μ rescatterings in the elastic amplitude. Consider, for example, a term in the elastic amplitude that involves three interactions, as shown in Fig. 1(a). Each wavy line represents an interaction, which in the Regge language corresponds to a Pomeron exchange. Cutting two of those Pomeron lines makes a contribution of the $\mu=2$ term in (3.3). The uncut line contributes to rescattering, and a sum of all uncut lines makes up the exponential factor in (2.11). Thus we need only consider the cut Pomerons, the exposure of which reveals the production amplitude. B_n^μ in (3.3) then expresses the probability of producing n particles when there are μ cut Pomerons, and $\pi_\mu(R)$ gives the weight for having μ cut Pomerons, when the scaled impact parameter is R .

The branching part of our model treats each cut Pomeron as a cascade of clusters. More explicitly, cutting a Pomeron term in the elastic amplitude means summing over production amplitudes squared, as depicted in Fig. 1(b); each production amplitude is treated as a cascade of clusters, as shown in Fig. 1(c). Different cascades corresponding to different cut Pomerons are independent of one another except that the initial energies E_i add up to \bar{W} , a constraint that is to be applied separately to every term in the series in (3.3). That is, for the μ th term in the series we have

$$E_i = e_i \bar{W}, \quad i = 1, 2, \dots, \mu, \quad (3.4)$$

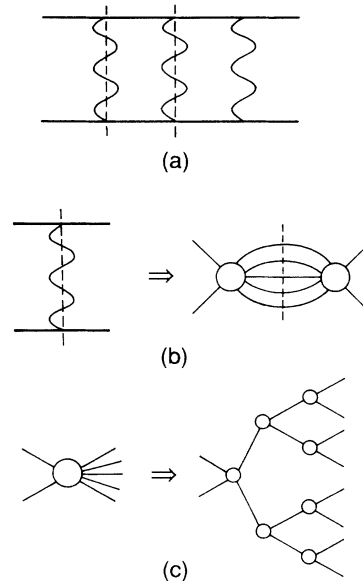


FIG. 1. (a) A three-Pomeron exchange contribution to the elastic-scattering amplitude with two cut Pomerons. (b) The relationship between a cut Pomeron and a sum over production processes. (c) A production process represented by branching subprocesses.

where e_i is a real number between 0 and 1, satisfying

$$\sum_{i=1}^{\mu} e_i = 1, \quad (3.5)$$

E_i is the c.m. energy of the i th cut-Pomeron term.

Since there is no theoretical prescription for the values of e_i , which is outside what Regge theory can specify, we choose in ECCO to regard e_i as a random number between 0 and 1, and to use μ such numbers constrained by (3.5) to specify E_i , $i = 1, \dots, \mu$. Since E_i is determined from \bar{W} , which is the mean value averaged over all events at R , the value of E_i cannot realistically be regarded as the initial energy of a cascade of clusters for a specific collision at R . As will become clear later, E_i will be used mainly to help determine the number of steps of the cascade.

C. First step in the cascade

In order to form a picture of the branching process, it is helpful to start with the parton model in mind. In the parton model quark and gluon distributions in a proton are Q^2 dependent; if Q^2 is small, say $Q \sim 2$ GeV/c, the distributions can be regarded as a description of the parton momenta appropriate for soft-interaction considerations. Indeed, Ochs [24] has observed many years ago that the parton momentum distribution is very similar to the inclusive pion distribution. It suggests that in soft collisions one may regard the partons in the opposite-going protons as having no interactions after the confinement bags are broken, and that they hadronize locally in rapidity space. This picture is, of course, too crude to be taken seriously. Nevertheless, the hint is that there is no long-range interaction among the partons

from the two incident protons, the rapidity separation among them being mostly very large, and that very short-range correlation in rapidity eventually leads to hadronization.

The hint suggests a general strategy in formulating the branching process in our model. We want branching because that is the only way we can get intermittency. We also want the eikonal formalism because it provides the solid foundation that will guarantee the global features to be correct in addition to having the proper connection to elastic scattering through unitarity. In that formalism the branching process can be introduced only as many cascading subprocesses acting in parallel, each having an “initial energy” E_i . To incorporate the suggestion hinted by the naive picture of the parton model, the first step in the cascade must not be into two massive clusters with opposite momenta determined by energy-momentum conservation, since that would introduce too much long-range correlation. As we have concluded in Sec. III A, energy conservation is meaningless when the total energy W for particle production is unknown from event to event.

Recognizing that the parton distribution is an average distribution, averaged over many events, we should not expect our cascade products to behave the same way for every event. Since the parton distribution has a rounded peak at zero-momentum fraction, the mapping from momentum fraction to rapidity yields a rapidity distribution that has a central flat plateau. The fluctuation of parton rapidities in the central region can be substantial from event to event so long as the sum reproduces the plateau structure of the inclusive distribution. With all this in mind we now prescribe the first step of the cascade. Regarding E_i as the mass m of the mother cluster that partitions into two daughter clusters of masses m_1 and m_2 , we require first that the mass distribution be

$$D(m_1, m_2) = \left[\frac{m_1 + m_2}{m} \right]^\gamma, \quad (3.6)$$

while the relative magnitude of m_1 and m_2 is totally random; γ is a parameter to be determined phenomenologically. Note that no mass scale is introduced in (3.6). The rapidities of m_1 and m_2 are $+y_1$ and $-y_2$, where y_i is a random number between 0 and y_{\max} with

$$y_{\max} = \zeta \ln(\sqrt{s}/m_p), \quad (3.7)$$

m_p being the proton mass, and ζ another parameter to be determined. The random distribution in y yields, upon event averaging, a flat plateau structure whose width depends on ζ .

An important part of the above prescription is that energy-momentum conservation is not imposed. As already mentioned, W is not known, neither are the momenta of the leading particles in every event. To keep track of the energy and momentum of each cluster is therefore pointless. In reality there may not be any clusters in the sense of timelike massive states with a reasonably well-defined notion of mass and momentum. The guide posts for our branching process will be intermittency, which is the phenomenology of fluctuations. We use

the language of clusters to implement our ideas about cascading in order to obtain intermittency. Our emphasis will be placed on where in rapidity the particles are likely to be produced relative to one another, and subject to that likelihood we must allow our branching system to fluctuate in all variables that can, in principle, fluctuate from event to event. At the end of the hadronization process we need only make sure that energy is conserved for the produced particles to the extent that W does not exceed $\sqrt{s} - 2m_p$. We shall calculate the distribution of W from the produced particles in all events and verify that $\langle W \rangle$ is roughly $\sqrt{s}/2$, as it should be. The fluctuation of W from $\langle W \rangle$ will be found to be large, also as we expect it to be.

D. Subsequent steps in the cascade

After the first step, the clusters m_1 and m_2 will act themselves as mothers and separately partition into two daughter clusters each in accordance to the mass distribution (3.6). The essential difference from the first step is in the rapidity distribution of the daughters. We assume that in all subsequent steps the rapidity y of a daughter relative to the rapidity of the mother satisfies a power-law distribution

$$p(y) = p_0 y^{-\beta}, \quad 0 \leq y \leq y_{\text{cut}}, \quad (3.8)$$

where

$$y_{\text{cut}} = \text{arccosh} \frac{m}{m_1 + m_2}, \quad (3.9)$$

and p_0 is a normalization factor with $\beta < 1$ being a new parameter. If one daughter has a positive y in the mother's rest frame, the other daughter has a negative y , independently generated according to (3.8). We do not require energy-momentum conservation at each subsequent step of the cascade for the same reason as we have given for the first step. Equation (3.8) is unlike any y distribution that one usually associates with hadron production, but $p(y)$ does not refer to observed hadrons. We propose this form for cluster decay mainly to avoid the introduction of any y scale (except for the finite-size effect associated with y_{cut}), while having short-range correlation that must be operative in the course of hadronization. For β positive, the two daughters can be very close in rapidity, thereby allowing the possibility of spikes in the final distribution, if a sequence of such close daughters are produced in succession. Such occurrences are rare, but then so are spike events [25]. The power law in (3.8) constitutes the kernel of our branching process that can give rise to self-similarity of observables under scale transformation of resolution in rapidity. Evidently, the dynamical mechanism of particle production is constructed here with hints gleaned from intermittency. Our tests on this mechanism are to check whether it can not only yield the correct rapidity fluctuations that are quantified by the intermittency analysis, but also generate the two-particle correlation distribution for the observed hadrons.

E. Hadronization

We terminate the cascade when the cluster mass reaches that of a pion. This is implemented in our code by the algorithm that so long as the cluster mass m is greater than $2m_\pi$, we allow it to decay further into two daughters according to (3.6) and (3.8). If $m < 2m_\pi$, we stop the cascade and identify the hadron as a pion, assigning it the mass m_π . This procedure does not exclude the possibility that a detected pion can be the decay product of a resonance, since the cluster before the last step of branching may well be a resonance. At this stage of the development of our code we choose the simplest procedure that can produce all the main features of the data. Thus we are ignoring kaon production, specific resonances, charge and spin, etc. All of these features will in time be incorporated into our code in later improved versions.

F. Transverse Momentum

After the branching process terminates in hadrons we can then ask about the values of the kinematic variables that are observed, in particular, y , W , and transverse momentum p_T . Since the simulation determines the values of y for all produced particles in every event, we can define a quantity that has the interpretation of longitudinal energy:

$$W_L = \sum_{i=1}^n m_\pi \cosh y_i, \quad (3.10)$$

where i is summed over all n hadrons (pions) that are produced. A weak form of energy conservation is

$$W_L < \sqrt{s} - 2m_p \quad (3.11)$$

which certainly should be satisfied. However, the transverse energy can also be substantial and must also be taken into account in the energy consideration.

In treating the transverse momenta of the produced hadrons we can take advantage of an important feature of the GBM, viz. the conjugate relationship between p_T and the overlap size based on the uncertainty principle. Clearly, the larger R is, the smaller is the overlap region of the two incident protons, and the larger is the fluctuation in p_T among the final pions produced. Since the overlap region of two spheres with fuzzy edges has a cumbersome geometrical dependence on the impact parameter, we use a simple Gaussian distribution to describe the overlap; the corresponding p_T distribution is then also a Gaussian with a width that depends on R , which we parametrize as

$$f(p_T, R) = f_0 \exp \left[-\frac{p_T^2}{2(\alpha R)^2} \right], \quad (3.12)$$

where f_0 is the normalization constant and α is a parameter characterizing the direct relationship between the mean p_T and R mentioned above. Thus in the GBM we have a p_T distribution for each R , and the observed p_T distribution involves an impact-parameter smearing.

In our code we first generate all the events without any

p_T . We discard all those events that violate (3.11). It turns out to be a very small fraction of the total number of events, as we shall see in the next section. Then in each collision, for which there is a definite value of R , we use (3.12) to generate p_T for all the particles produced in the event. From the y_i and p_{T_i} of the i th particle, we can calculate

$$W = \sum_{i=1}^n (m_\pi^2 + p_{T_i}^2)^{1/2} \cosh y_i \quad (3.13)$$

for that event. Energy conservation now requires

$$W < \sqrt{s} - 2m_p. \quad (3.14)$$

A small fraction of events may violate this, although every event satisfies (3.11) before p_T is introduced. Those events that violate (3.14) are then required to have $p_T = 0$ for all particles produced. In this way we retain all events that satisfy (3.11), and use energy conservation (3.14) to limit the p_T of particles with large W_L . This would result in an increase of $d\sigma/dp_T$ in the first p_T bin which is, however, experimentally inaccessible.

IV. RESULTS OF ECCO

There are five adjustable parameters in ECCO. The eikonal function is an external input fixed by elastic scattering, and is therefore not adjustable. The five parameters are λ , γ , ξ , β , and α , introduced in (3.2), (3.6), (3.7), (3.8), and (3.12), respectively. We shall determine them by fitting the NA22 data at $\sqrt{s} = 22$ GeV, and then with those parameters fixed we let \sqrt{s} run from 10 to 65 GeV. To be able to fit a vast variety of data with just five parameters is an indication of how good the GBM is.

The parameter λ , which controls the average energy \bar{W} of particle production at R , has a strong effect on the average multiplicity $\langle n \rangle$. To have KNO scaling is an anticipated virtue of the GBM, based on the results of previous work [1]. The number of steps of the cascade is controlled by the parameter γ , which, together with λ , strongly affects the fluctuations of the multiplicities from the average $\langle n \rangle$. The degree of those fluctuations are described by the normalized moments

$$C_q = \langle n^q \rangle / \langle n \rangle^q, \quad (4.1)$$

where

$$\langle n^q \rangle = \sum_n n^q P_n. \quad (4.2)$$

The shape of the single-particle rapidity distribution

$$\rho_1(y) = \frac{dn}{dy} \quad (4.3)$$

is particularly dependent on ξ and β , since ξ influences the width of the plateau through y_{\max} , and β affects the width of the decay in each step of the cascade. Even more sensitive to β is the two-particle distribution

$$\rho_2(y_1, y_2) = d^2n / dy_1 dy_2, \quad (4.4)$$

or more specifically the correlation function

$$C(y_1, y_2) = \rho_2(y_1, y_2) - \rho_1(y_1)\rho_1(y_2), \quad (4.5)$$

as well as higher-order correlations. We shall actually determine β mainly by examining the normalized factorial moments [9,10]

$$F_q = \frac{1}{M} \sum_{j=1}^M \frac{\langle k_j(k_j-1) \cdots (k_j-q+1) \rangle}{\langle k_j \rangle^q}, \quad (4.6)$$

where k_j is the multiplicity of particles in the j th bin and M is the total number of bins in the rapidity interval Y , i.e.,

$$M = Y/\delta, \quad (4.7)$$

δ being the bin width. The average $\langle \cdots \rangle$ in (4.6) is taken over all the events for the j th bin. The F_q thus obtained in (4.6) are referred to as vertically analyzed factorial moments, horizontally averaged.

Since we have not kept track of the charge states, n_{ch} is taken simply to be $2n/3$, where n is the total multiplicity of produced particles. NA22 has provided the most exhaustive data on a wide variety of observables [26], but unfortunately at only $\sqrt{s} = 22$ GeV. We regard those data as our benchmark, and determine all our parameters by fitting their data points. We let the energy dependence be a prediction. Since only soft interaction is considered in this code, we vary \sqrt{s} only in the range 10–65 GeV now, adding hard collisions later to extend the validity of the model to the CERN SPS collider energy range and beyond [12].

For global features in the full rapidity space, NA22[26] lists the following values for the first four moments of the charge-multiplicity distribution in pp collisions:

$$\begin{aligned} \langle n \rangle &= 8.93 \pm 0.16, \\ C_2 &= 1.18 \pm 0.01, \\ C_3 &= 1.59 \pm 0.04, \\ C_4 &= 2.4 \pm 0.1. \end{aligned} \quad (4.8)$$

ECCO can fit them all with the choice of the two parameters

$$\lambda = 0.1, \quad (4.9a)$$

$$\gamma = 0.3. \quad (4.9b)$$

We then let \sqrt{s} vary from 10 to 65 GeV, and have calculated C_5 as well. The results are shown as dashed lines in Figs. 2 and 3. All predictions are within one standard deviation from the data at other energies [27]. In Fig. 3 all points are above our predictions because the NA22 points at 22 GeV are all low compared to the results from the other experiments. We can perform a best fit to all the data points at all energies. The results are shown as solid lines in Fig. 2 and 3. The corresponding values of the parameters are

$$\lambda = 0.1, \quad (4.10a)$$

$$\gamma = 0.2. \quad (4.10b)$$

The fits are evidently very satisfactory, and are particu-

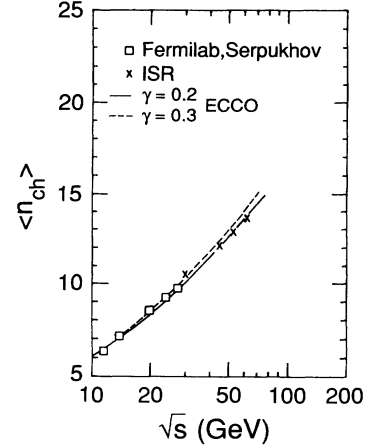


FIG. 2. Energy dependence of average charge multiplicity. Data are from Ref. [27]. The solid line is a fit of all data points by ECCO; the dashed line is a fit of only the NA22 data at $\sqrt{s} = 22$ GeV.

larly remarkable when one considers that only two parameters have been used in the fit.

Having achieved a good fit of the C_q moments, it would not be surprising to find that our prediction for P_n agrees perfectly with the data. In Fig. 4 we show the KNO plot of the multiplicity distribution [19]; the solid line is the calculated result using the parameters in (4.10). The data are for all energies at the CERN ISR [27].

For ζ and β we consider the data of NA22 on intermittency [26]. In Fig. 5 the factorial moments F_q vs δ in the log-log plot for $q = 2, \dots, 5$ are shown. All of the moments are fitted by the choice

$$\zeta = 0.75, \quad (4.11a)$$

$$\beta = 0.6. \quad (4.11b)$$

The results are shown by the solid lines in Fig. 5, for which (4.9) has been used for λ and γ , since they were

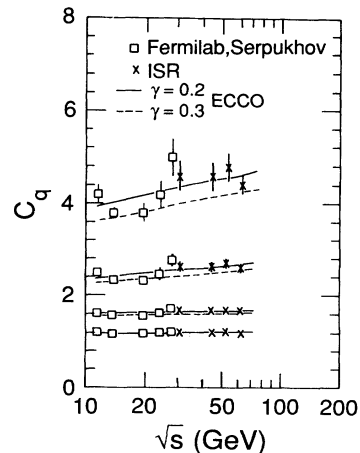


FIG. 3. Energy dependence of normalized moments C_q . Data and lines are as described in Fig. 2.

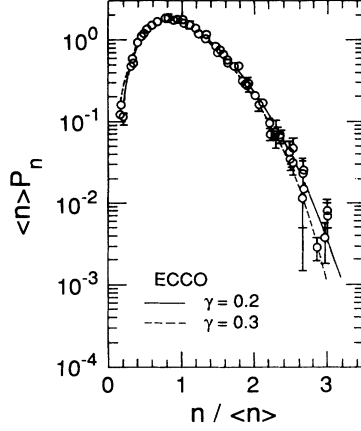


FIG. 4. KNO distribution. Data and lines are as described in Fig. 2.

determined by the NA22 data also. In the simulation 6×10^4 events have been used in keeping with the statistics of the data. Evidently, the fits are very good. The result is stable when other runs of 6×10^4 events or more are made. The value of ζ is actually determined primarily by the requirement that the single-particle rapidity distribution, dn/dy , has the proper shape, i.e., very nearly flat between $y = \pm 2$, and rather steep drop beyond that range. Figure 6 shows that distribution. No data is shown in that figure because the ISR data [28] were given in pseudorapidity η , and the recent NA22 data do not include dn/dy for pp collision. However, our result for dn/dy looks very good by comparing it with the ISR data at large η and with the NA22 data [26] on $\langle n \rangle$ at various y_{cut} .

The power-law behavior of F_q in Fig. 5,

$$F_q \propto \delta^{-\phi_q}, \quad (4.12)$$

exhibits the self-similarity of multiplicity fluctuation,

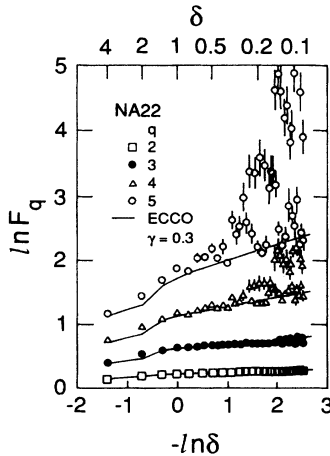


FIG. 5. Intermittency plot of F_q vs δ . Data are from Ref. [26]; the solid lines are from ECCO using (4.9) and (4.11).

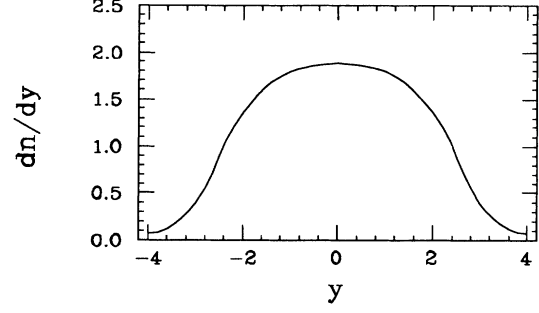


FIG. 6. Average rapidity distribution at 22 GeV from ECCO.

where δ is lowered from 4 to 0.1. In our model this is achieved by the $p(y)$ distribution of (3.8), which describes the daughter rapidities that peak at small y without a scale. As far as we know, the GBM as implemented by ECCO described here is the only dynamical model on soft production in hadronic collisions that can yield results in agreement with the intermittency data. The intermittency indices ϕ_q are shown in Fig. 7. The anomalous fractal dimension

$$d_q = \frac{\phi_q}{q-1} \quad (4.13)$$

increases with q , as shown in Fig. 8. This is a characteristic feature of the hadronic collisions, where d_q increases with q .

Since momentum conservation has not been imposed during branching, and since the power-law rapidity distribution (3.8) for cluster decay is not familiar, it is useful to determine the two-particle correlation function of the produced particles, (4.5), which is far more familiar. This is shown in Fig. 9, which represents 11×10^4 events having $n = 15$ and 16, out of a total of 10^6 events. It is an exclusive correlation function $C_n(y_1, y_2)$ in that only events with n particles are considered. When integrated over both y_1 and y_2 , it is normalized to $-n$, but when y_1 is fixed at 0, the integration over y_2 yields $-\rho_1(0)$. Figure 9 shows the correct shape with correlation length around

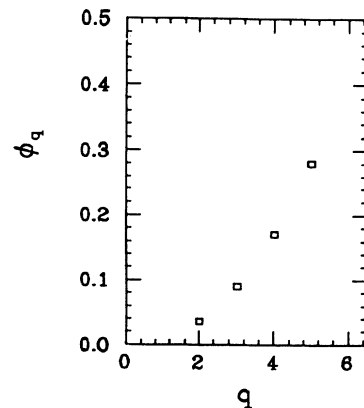


FIG. 7. The intermittency indices as a function of the order q of the moments.

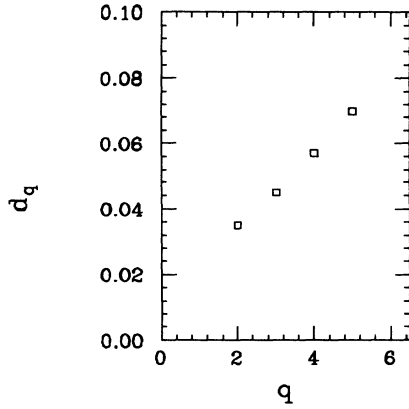


FIG. 8. The anomalous fractal dimension d_q as a function of q .

one unit of rapidity. Since we do not yet have predictions on charged particle spectra, we cannot compare our results quantitatively with the data on charged-particle correlation functions [29]. There being no adjustable parameter used here, we feel that our results are qualitatively satisfactory. It should be emphasized that, unlike many models where two-particle correlation is put in by hand with adjustable correlation length ξ , we calculate $C(y_1, y_2)$ from the dynamical process of branching, and that the observed $\xi \approx 1$ is an output from our simulation by ECCO.

It is worthwhile to remark that to fit the factorial moments in Fig. 5 does not necessarily imply that one must subscribe to the view in favor of the existence of a new physics underlying the power-law behavior. Indeed, there are some [30] who stress that the conventional short-range correlation is enough to fit the data on F_q . However, we believe that the challenge has been to construct a dynamical model that can fit the data in Fig. 5. We have found the task difficult until (3.8) is adopted and positive β tried. We note that $p(y) \propto y^{-0.6}$ is a rather broad distribution, but also has a singularity at $y=0$; it represents the essence of the “new” physics that ECCO

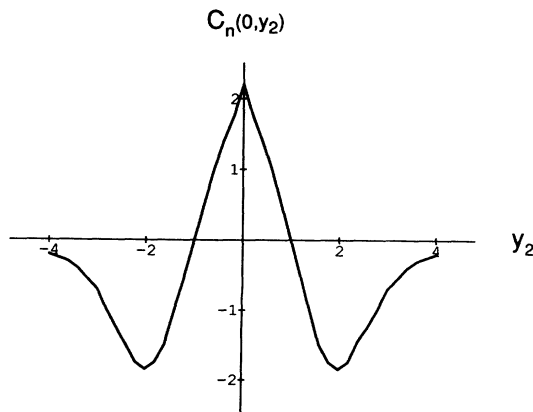


FIG. 9. Two-particle correlation function, defined in (4.5), with y_1 fixed at 0.

has uncovered.

For the p_T distribution it is well known that the average transverse momenta of soft production in the ISR range is $\langle p_T \rangle \approx 0.35$ GeV [29]. We have adjusted the parameter α in (3.12) to the value

$$\alpha = 0.4 \text{ GeV} \quad (4.14)$$

and obtained the final distribution dN/dp_T^2 of the produced particles that is exponential in p_T in the range $0.2 < p_T < 1$ GeV, i.e.,

$$dN/dp_T^2 \sim \exp(-p_T/p_{T0}). \quad (4.15)$$

The result is shown in Fig. 10 and compared with the ISR data [29] for $p+p \rightarrow \pi^\pm + X$, which have $\langle p_T \rangle = 0.35$ GeV; the normalization is adjusted to fit, since the data are for $Ed^3\sigma/dp^3$ at $y_{\text{lab}} = 1.5$. The solid lines in that figure are for $\sqrt{s} = 22$ GeV, while the dotted lines are for $\sqrt{s} = 63$ GeV, for which we have repeated the calculation with exactly the same parameters. Our dN/dp_T^2 has a small increase at $p_T = 0$ because 15% of the events are required to have no p_T in order to satisfy (3.14). Although the effect at $p_T = 0$ is not observable, it is nevertheless an unsatisfactory aspect of the code that we hope to remove in an improved version later, when branching in three dimensions is considered. The value of α in (4.14) is physically reasonable since R varies from zero at complete overlap to essentially 2 where $\Omega(R)$ is less than 1% of $\Omega(0)$.

Finally, we can calculate the W distribution. In our simulation initially with p_T set to zero we found that although energy-momentum conservation has not been applied during cascading, only 1.5% of the events have W_L that violates (3.11). Those events are rejected. The results in Figs. 2–10 do not include those events. For the

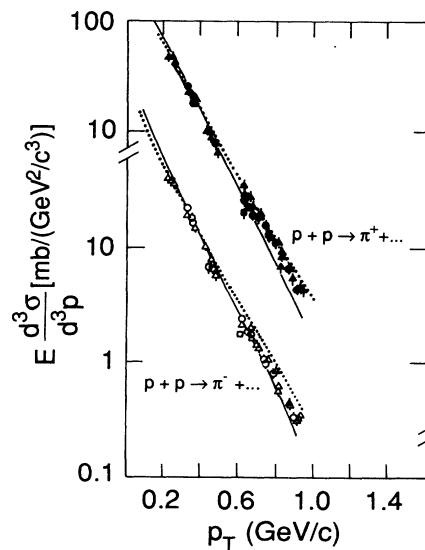


FIG. 10. Transverse-momentum distribution with data from Ref. [29] and solid line (22 GeV) and dotted line (63 GeV) from ECCO. The data are for $y_{\text{lab}} = 1.5$, so the normalizations of the lines are adjusted to fit the data at $p_T = 0.4$ GeV/c.

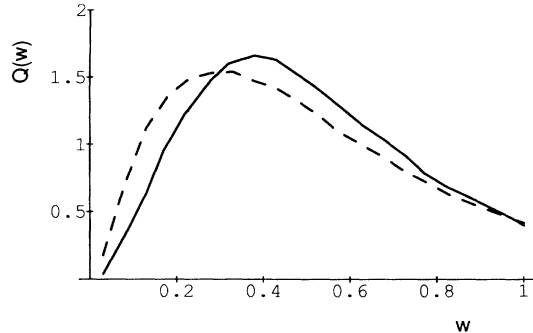


FIG. 11. Distribution of energy fraction for particle production at 22 GeV (solid line) and 63 GeV (dashed line).

remaining 98.5% events we introduce p_T in accordance to the procedure given in Sec. III F with results described in the preceding paragraph. Knowing y_i and p_{T_i} for each particle in each event, we can calculate W according to (3.13). For the W distribution of all events, we introduce the scaled variable

$$w = W/(\sqrt{s} - 2m_p) \quad (4.16)$$

and give the normalized w distribution $Q(w)$ in Fig. 11 for $\sqrt{s} = 22$ and 63 GeV. The average fraction of energy for particle production is $\langle w \rangle = 0.51$ for $\sqrt{s} = 22$ GeV, and 0.46 for $\sqrt{s} = 63$ GeV. This is in accord with the empirical notion that inelasticity is around $\frac{1}{2}$ and decreases with energy.

We find all the results obtained to be very satisfactory. Since every feature of multiparticle production, global as well as local, is reproduced in our simulation, we feel that the GBM must have captured the essence of soft-production processes.

V. CONCLUSION

We have shown that ECCO is able to produce correctly all the global and local features of particle production in soft hadronic collisions in the energy range $10 \leq \sqrt{s} \leq 65$ GeV. The success is to be traced to both the geometrical aspect of the model, which is implemented by the eikonal formulation of hadronic collisions, and the dynamical aspect that is contained in the branching process. While the eikonalism is standard and general, the branching dynamics for soft interaction is not. It is not fashioned after hard collisions, nor is it purely stochastic. It could not have been devised without the guidance of intermittency. In that respect the large body of experimental work on intermittency has been fully justified.

The physical picture of the production process that we gain from this study is not a simple one, as it should not be, since hadrons are complicated, extended objects. The eikonal formalism orders the inelastic collision process in a series of basic interactions; the number of important terms in that series depends on the impact parameter R . The smaller R is, the more overlap, and the more interactions take place. Unless the experiment makes special cuts to select the centrality of the collisions, R must be

integrated over, and therein lies an important source of fluctuation that must not be overlooked.

After the whole collision is reduced to a series of basic interactions, our attention can then be focused on the nature of the interaction that leads to particle production. Although we used the language of cluster cascading, the clusters have not been treated as massive objects on mass shells. The masses that have been given them have been used only for the purpose of tracking the evolution of branching. Playing the role of time in more conventional stochastic processes, those masses act as evolution parameters and determine when the various cascading chains stop branching. If we think in terms of partons, we can always group partons in a certain portion of the phase space together and call them clusters. By not requiring those massive clusters to decay with energy-momentum conservation, we are effectively allowing the partons to be off shell, while they evolve toward hadronization.

The dynamical content of our branching process is that in the first step the left-going and right-going partons are uncorrelated and can essentially be anywhere in the rapidity space. But after that, the clustering of partons has no preferred scale of rapidity separation. This results in the short-range correlation in the produced hadrons observed globally. More than that, it also allows the particles to be very close in rapidity, thereby providing the possibility of spike events, which are rare but cannot be totally absent, if the self-similarity of rapidity fluctuation extends down to very small bin size.

The success of ECCO should not be taken to imply that we understand fully the real dynamics of soft production. We have found an effective method to describe the production process; however, to provide a more fundamental description of the dynamics that validates the procedure used in ECCO will require far more work yet to be done. At least we now have a direction to aim that we know is phenomenologically pertinent.

In addition to including jet production at higher energies, a very urgent development to pursue with what we now have at hand is to apply ECCO to relativistic heavy-ion collisions, where new data are abundant. We see no basic difficulty in doing that, since the generalization of the eikonal formalism to nuclear collisions has already been considered [13]. If the intermittency data of heavy-ion collisions can be reproduced by ECCO without further adjustment, then what we have at hand is an effective tool to detect any basic change in the nuclear medium that may occur in the future, when either the nuclear size or the energy is increased. For if the formation of quark-gluon plasma leads to a different intermittency pattern [31], then ECCO should fail to fit the data in the new regime, and that failure would be a signal of new physics.

ACKNOWLEDGMENTS

We would like to thank X. N. Wang for helpful discussions. This work was supported in part by the U. S. Department of Energy under Grants Nos. DE-FG06-85ER-40224 and DE-FG06-91 ER40637.

- [1] W. R. Chen and R. C. Hwa, *Phys. Rev. D* **36**, 760 (1987); W. R. Chen, R. C. Hwa, and X. N. Wang, *ibid.* **38**, 3394 (1988).
- [2] For a review, see R. C. Hwa, in *Hadronic Matter in Collision*, Proceedings of the Second International Workshop on Local Equilibrium in Strong Interaction Physics, Tucson, Arizona, 1988, edited by P. Carruthers and J. Rafelski (World Scientific, Singapore, 1989); in *Relativistic Heavy-Ion Collisions*, edited by R. C. Hwa, C. S. Gao, and M. H. Ye (Gordon and Breach, London, 1990).
- [3] W. R. Chen, R. C. Hwa, and X. N. Wang, *Phys. Rev. D* **43**, 2425 (1991).
- [4] A. Capella, U. Sukhatme, C. I. Tan, and J. Tran Thanh Van, *Phys. Lett.* **81B**, 68 (1979); A. Capella, R. Sukhatme, and J. Tran Thanh Van, *Z. Phys. C* **3**, 329 (1980); G. Cohen-Tannoudji *et al.*, *Phys. Rev. D* **21**, 2689 (1980).
- [5] A. Capella and J. Tran Thanh Van, *Z. Phys. C* **23**, 165 (1984); A. Capella, A. Staar, and J. Tran Thanh Van, *Phys. Rev. D* **32**, 2933 (1985); A. Kaidalov and K. A. Ter-Martirosian, *Phys. Lett.* **117B**, 247 (1982); A. Aurenche, F. Bopp, and J. Ranft, *ibid.* **147B**, 212 (1984); T. Kanki, *Nucl. Phys.* **B243**, 44 (1984).
- [6] B. Andersson, G. Gustafson, and B. Nilsson-Almqvist, *Nucl. Phys.* **B281**, 289 (1987); B. Nilsson-Almqvist and El. Stenlund, *Phys. Commun.* **43**, 387 (1987).
- [7] For a broad review of various models, see *Hadronic Multiparticle Production*, edited by P. Carruthers (World Scientific, Singapore, 1988).
- [8] For a review, see *Intermittency in High Energy Collisions*, Proceedings of the Santa Fe Workshop, Los Alamos, New Mexico, 1990, edited by F. Cooper, R. C. Hwa, and I. Sarcevic (World Scientific, Singapore, 1990).
- [9] A. Bialas and R. Peschanski, *Nucl. Phys.* **B273**, 703 (1986); **308**, 857 (1988).
- [10] W. Kittel, in *Proceedings of the 20th International Symposium on Multiparticle Dynamics*, edited by R. Baier and D. Wagener (World Scientific, Singapore, 1991).
- [11] T. Sjostrand and M. Bengtsson, *Comput. Phys. Commun.* **43**, 367 (1987); T. Sjostrand, *Int. J. Mod. Phys. A* **3**, 751 (1988); T. Sjostrand, *JETSET7.3* (1990).
- [12] R. C. Hwa, *Phys. Rev. D* **37**, 1830 (1988); W. R. Chen and R. C. Hwa, *ibid.* **39**, 179 (1989); X. N. Wang and R. C. Hwa, *ibid.* **39**, 187 (1989).
- [13] R. C. Hwa and X. N. Wang, *Phys. Rev. D* **39**, 2561 (1989); **42**, 1459 (1990).
- [14] J. Dias de Deus, *Nucl. Phys.* **B59**, 231 (1973); A. J. Buras and J. Dias De Deus, *ibid.* **B71**, 481 (1974).
- [15] T. T. Chou and C. N. Yang, *Phys. Rev.* **170**, 1591 (1968); *Phys. Rev. Lett.* **20**, 1213 (1968); L. Durand and R. Lipes, *ibid.* **20**, 637 (1968); R. J. Glauber, in *Lectures in Theoretical Physics*, edited by W. E. Brittin and L. G. Dunham (Interscience, New York, 1959), Vol. 1; R. J. Glauber and G. Mathiae, *Nucl. Phys.* **B21**, 135 (1970).
- [16] V. V. Anisovich, M. N. Kobrinsky, J. Nyiri, and Yu. M. Shabelski, *Quark Model and High Energy Collisions* (World Scientific, Singapore, 1985).
- [17] R. C. Hwa, in *Hadronic Multiparticle Production* [7].
- [18] W. H. Furry, *Phys. Rev.* **52**, 569 (1937); C. S. Lam and M. A. Walton, *Phys. Lett.* **140B**, 246 (1984); D. C. Hinz and C. S. Lam, *Phys. Rev. D* **33**, 3256 (1986).
- [19] Z. Koba, H. B. Nielsen, and P. Olesen, *Nucl. Phys.* **B40**, 317 (1972). The experimental evidence for KNO scaling can be found in the collected data in Ref. [27].
- [20] R. C. Hwa, *Nucl. Phys.* **B328**, 59 (1989).
- [21] C. B. Chiu and R. C. Hwa, *Phys. Lett. B* **236**, 466 (1990); and in *Intermittency in High Energy Collisions* [8].
- [22] A. W. Chao and C. N. Yang, *Phys. Rev. D* **8**, 2063 (1973).
- [23] E. W. Anderson *et al.*, *Phys. Rev. Lett.* **19**, 198 (1967); M. A. Abolins *et al.*, *ibid.* **25**, 126 (1970); D. S. Barton *et al.*, *Phys. Rev. D* **27**, 2580 (1983).
- [24] W. Ochs, *Nucl. Phys.* **B118**, 397 (1977).
- [25] M. Adamus *et al.*, *Phys. Lett. B* **185**, 200 (1987).
- [26] W. Kittel, in *Hadronic Multiparticle Production* [7]; M. Adamus *et al.*, *Z. Phys. C* **37**, 215 (1988); I. V. Ajinenko *et al.*, *Phys. Lett. B* **222**, 306 (1989); **235**, 373 (1990); H. Bottcher *et al.*, Nijmegen Report No. HEN-334/90, 1990 (unpublished).
- [27] G. J. Alner *et al.*, *Phys. Lett.* **160B**, 193 (1985); **167B**, 476 (1986).
- [28] W. Thome *et al.*, *Nucl. Phys.* **B129**, 365 (1977).
- [29] G. Giacomelli and M. Jacob, *Phys. Rep.* **55**, 1 (1979).
- [30] A. Capella, F. Fialkowski, and A. Krzywicki, *Phys. Lett. B* **230**, 149 (1989); P. Carruthers and I. Sarcevic, *Phys. Rev. Lett.* **63**, 1562 (1989); P. Carruthers, H. C. Eggers, and I. Sarcevic, *Phys. Lett. B* **254**, 258 (1991).
- [31] A. Bialas and R. C. Hwa, *Phys. Lett. B* **253**, 436 (1991).